AERODYNAMIC SHAPE OPTIMIZATION OF GUIDED MISSILE BASED ON WIND TUNNEL TESTING AND CFD SIMULATION

by

Goran J. Ocokoljić[a], Boško P. Rašuo[b*], and Aleksandar Bengin[b]

[a] Military Technical Institute, Belgrade, Serbia

[b] University of Belgrade, Faculty of Mechanical Engineering, Belgrade, Serbia

This paper presents modification of the existing guided missile which was done by replacing the existing front part with the new five, while the rear part of the missile with rocket motor and missile thrust vector control system remains the same. The shape of all improved front parts is completely different from the original one. Modification was performed based on required aerodynamic coefficients for the existing guided missile. The preliminary aerodynamic configurations of the improved missile front parts were designed based on theoretical and Computational Fluid Dynamics simulations. All aerodynamic configurations were tested in the T-35 wind tunnel at the Military Technical Institute (VTI) in order to determine the final geometry of the new front parts. Three-dimensional Reynolds Averaged Navier–Stokes numerical simulations were carried out to predict the aerodynamic loads of the missile based on the finite volume method. Experimental results of the axial force, normal force and pitching moment coefficients are presented. The computational results of the aerodynamic loads of a guided missile model are also given, and agreed well with.

Key words: *experimental aerodynamics, wind tunnel testing, CFD, aerodynamic coefficients, missile model*

1. Introduction

Modern missile configuration designs tend to reduce the area of control surfaces, such as fins and tails, in order to achieve better aerodynamic performance characteristics in flight. As a result of these design requirements, stability problems could appear at the speed in the low subsonic regime. For this case, the wing-store interference and low controllability may cause serious safety problems. Therefore, investigations of the flow field over missile configurations at the subsonic flow and understanding of the effect that control surfaces have on the stability characteristics and the development of flow asymmetries are crucial to efforts in improving the design of future-generation missiles. In all phases of a missile design it is necessary to know the aerodynamic coefficients as a function of the angle of attack for different Mach numbers and control deflections. In the preliminary design, an accurate prediction of the aerodynamic coefficients is necessary for the choice of aerodynamic configuration.

The process of missile design requires the use of a variety of theoretical, experimental and numerical methods [1],[2]. The experiment comprises the measurement of aerodynamic forces and moments on the model in the wind tunnel. The Computational Fluid Dynamics (CFD) simulations play an important role in eliminating preliminary models at the beginning of the design process and leaving expensive wind tunnel testing for detailed models that are close to the final design.

* Corresponding author, e-mail address: brasuo@mas.bg.ac.rs Tel: +381638676773

This paper presents such a combined experimental and numerical approach to a modification of an existing guided missile. The original configuration of the missile comprised a shaped-charge warhead that was to be replaced by a choice of five new, more effective, warheads, while the rear part of the missile with the rocket motor and missile thrust vector control system were to remain unchanged. As the aerodynamic shapes, masses and the positions of the centers of gravity of the new warheads differed significantly from the shape of the original one, substitutions of the warhead would have resulted in the changes of the aerodynamic characteristics of the missile. There was a requirement, however, to retain the existing semiautomatic command guidance and missile control system, which required that the aerodynamic characteristics of the modified missiles had to remain similar to the original one. This was to be achieved by placing additional aerodynamic surfaces on the front part of the missiles (i.e. on the new warheads). The new aerodynamic surfaces were to be sized and positioned so as to return C_{N_α} and C_{m_α} close to the original ones in order that the modified configurations have the same (or slightly better) maneuverability as the original missile, with a minimum penalty of drag increase. Several variants of these additional surfaces were designed for each of the new warheads, and the designs analyzed in CFD simulations. Optimization and selection of the final geometries of the five new front parts of the missile on the basis of the lift-curve and pitching-moment-curve slopes and lift/drag ratio decrease were then performed in the wind tunnel testing.

2. Experiment

The data for this investigation was obtained in the T-35 subsonic wind tunnel of VTI. The wind tunnel is of continual type, closed-circuit facility and capable of operation at a Mach number range of 0.1<M<0.5 at atmospheric pressure, **Error! Reference source not found.**,[3],[4]. The wind tunnel is equipped **Error! Reference source not found.**,[5],[5] with two removable solid wall test sections, first, a general purpose test section with an external six-component balance/model support and, second, a test section with a tail sting support system. Each test section has an octagonal cross-section, with a larger axis of 4.4m and a smaller axis of 3.2m. Cross- sectional area is 11.93m^2. The length of each test section is 5.5m.

Figure 1. Two parts of the original model: the rocket body and the front part.

Figure 2. The 2M Model.

The Mach number regulation is achieved by changing the fan rotation rate and the angle of fan blades. The value of Reynolds number is up to 12 million/m with a fan. The value of the total pressure in the test section is 1 bar. Theoretically, the duration of the test is unlimited. The facility is used for research projects as well as for educational experiments and demonstrations. The GM model shown in this paper is composed of the front part located in the front part and the rocket motor with the thrust vector control systems located in the rear part of the missile. Figure 1 presents the Original GM model

parts. The original model and the modified versions, named 2M, 2T, 2F, 2TT and 2FF model, were designed and tested in the T-35 wind tunnel. Figure 2 shows the 2M model in the T-35.

Figure 3. The 2T Model.

Figure 4. The 2F Model.

Various models used in the investigation are shown in Figure 3 – Figure 6. These figures depict the five models, each with a different front part, each of the five parts has sets of wings that were used.

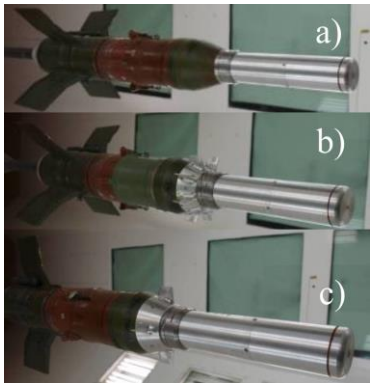

Figure 5. The 2TT model, a)without wings, b)with 8 wings and c) with 4 wings.

Figure 6. The 2FF model.

Figure 3 and Figure 4 show the 2T and 2F models mounted in the T-35 test section, respectively. Figure 5 and Figure 6 present the 2TT and the 2FF model mounted in the T-35 test section. The model was made from steel and aluminium alloy. Its main part is the body (wing section) made from steel. The model body was designed for the setting of the internal wind tunnel balance. The model was mounted on a sting. The origin of the wind axes system was in the model reference point [8].

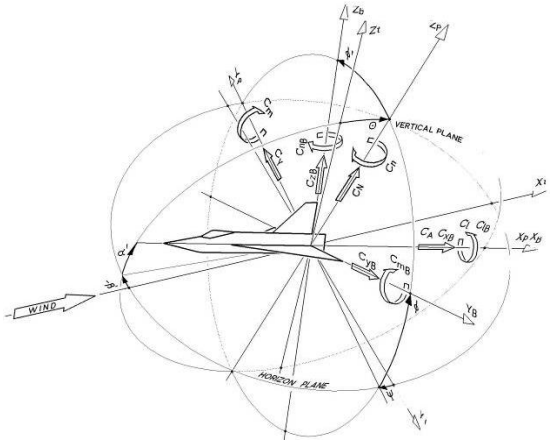

Figure 7. Axes systems used in data reduction.

Figure 7 shows the relative positions of these axes systems. A comparative survey of the basic dimensions of all tested models is given in Table 1.

Table 1. Basic dimensions

Front part type		Original	2M	2T	2F	2TT	2FF
Length,m	L	0.832	1.097	1.261	0.972	1.018	0.832
Diameter,m	D	0.120	0.120	0.120	0.120	0.120	0.120
Wing span,m	b	0.393	0.393	0.393	0.393	0.393	0.393
Referent length,m	D	0.120	0.120	0.120	0.120	0.120	0.120
Distance beetwen point of reduction and front of model, m	X_r	0.499	0.711	0.8555	0.5616	0.643	0.457
Referent area,m^2	S_{ref}	0.011304	0.011304	0.011304	0.011304	0.011304	0.011304

3. CFD Simulation

The numerical calculations of aerodynamic characteristics of the Original, 2M, 2T and 2F models, performed using the CFD methods prior to the wind tunnel test campaign, were necessary in order to estimate the expected loads on the wind tunnel model. The numerical calculation was done in the FLUENT package, as it allows calculation of the aerodynamic characteristics of complex aerodynamic shapes [9]-[19]. The solid model of the missile is done in INVENTOR software. Small details like a gap in the wings, attachments, which do not have a significant effect on aerodynamics, were removed/approximated for the CFD simulation. Nozzles and tracer that have had significant effect on the drag calculations are present. Control volume in the shape of an ellipsoid with a major axis three times greater than the length of the missile (3.8m) and a minor axis sixteen times greater than the missile diameter (1.9m) and length 5.5m was done by software GAMBIT with the boundary surface type ''pressure far field''. The computational domain inlet is located 15 model body diameter upstream from the tip of the model nose and the computational domain outlet is located 17 model body diameter downstream from the model base. Boundary conditions are Mach number, total pressure, total temperature and turbulence parameters corresponding to the values measured in the wind tunnel. All model body surfaces are of the ''wall'' type. The unstructured mesh composed of tetrahedral elements is generated in the control volume. The density-based, explicit, compressible, unstructured-mesh solver was used. A modified form of the k- ε two-equation turbulence model (realizable k- ε) was used in this study. This turbulence model solves transport equations for the turbulence kinetic energy, k, and its dissipation rate, ε. In most cases, the computation was initially done on a coarse mesh with a non-dimensional distance from the model of $y+\approx30$ in order to obtain the flow field that presented a basis for the grid adaptation. Mesh was generated with respect to selected mesh growth rate of 1.08, but mentioned growth rate parameter was chosen to vary up to the value of 1.2. Selection of appropriate growth rate parameter value directly affects total grid size. The finest grid was defined with total cells number of 2.6 million elements, which corresponds to the growth rate parameter of 1.08 and with the first wall node placed at $y+\approx1$ in the whole domain for the angles of attack. This density of the mesh was selected with respect to the sufficient amount of computer memory and convergence criteria of the calculated aerodynamic coefficients and residuals. It should be noted that a grid with the total number of cells of about 2.6 million was found to be sufficient to obtain a good agreement with test results and to ensure convergence of the calculated aerodynamic coefficients and residuals. Finer grids, between 2.6 million and 4 million elements, ensured a grid-independent solution. The near-wall region was discretized with 23 layers of prismatic cells, while the rest of the flow domain consisted of tetrahedral cells. In the regions where $y+\approx1$, the viscous sub-layer was resolved using a two-layer model for enhanced wall treatment, while the enhanced wall treatment through the blending of linear and logarithmic laws in the near-wall region was used in the regions with a higher y+. The cross-sections of the mesh in the computational domain for the 2M model is given in Figure 8.

The FLUENT commercial flow solver was used to compute the axial and normal force and pitching moment coefficients and flow-field around the missile model. The viscous computational fluid dynamic simulations were used to calculate the flow-field around the projectile model in subsonic flows. The FLUENT (v6.2.16) commercial flow solver is used to compute the base pressure values and the flow-field around the ATM model. The implicit, compressible, unstructured-mesh

solver is used. The three-dimensional, time-dependent, Reynolds-Average Navier-Stokes (RANS) equations are solved using the finite volume method (1) and (2):

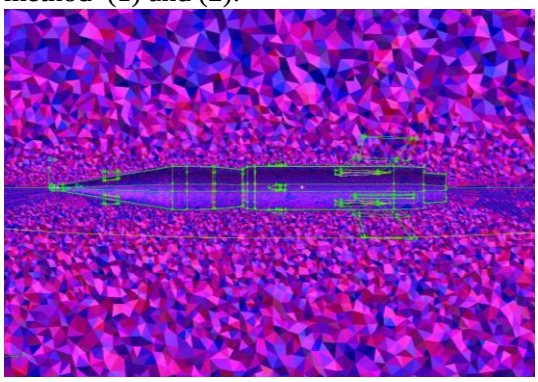

$$\frac{\partial}{\partial t}\int_V W dV + \oint [F - G] d\vec{A} = \int_V H dV \qquad (1)$$

where are

$$W = \begin{Bmatrix} \rho \\ \rho u \\ \rho v \\ \rho w \\ \rho E \end{Bmatrix}, F = \begin{Bmatrix} \rho v \\ \rho v u + pi \\ \rho v v + pj \\ \rho v w + pk \\ \rho v E + pv \end{Bmatrix}, G = \begin{Bmatrix} 0 \\ \tau_{xi} \\ \tau_{yi} \\ \tau_{zi} \\ \tau_{ij} + q \end{Bmatrix} \qquad (2)$$

Figure 8. Cross-section of the mesh in the 2M model vicinity.

The inviscid flux vector *F* is evaluated by a standard upwind flux-difference splitting. In the implicit solver, each equation in the coupled set of governing equations is linearized implicitly with respect to all dependent variables in the set, resulting in a block system of equations. A block Gauss-Seidel point implicit linear equation solver is used with an algebraic multigrid method to solve the resultant block system of equations. The computations were performed for the Mach number 0.35 at and the angle of attack from –10º to 10º. Convergence was determined by tracking the change in the flow residuals and the aerodynamic coefficients during the solution. The solution was deemed converged when the flow residuals were reduced at least 2 orders of magnitude and the aerodynamic coefficients changed less than about 2% over the last 100 iterations.

4. Results

In order to fulfill the requested ratio between the pitching moment and the normal force coefficients, the wings are added on the forward part of the missile where the front part is located. The aim of the experiment was to determine the configurations of the wings such that for the same normal force coefficients as the Original GM get the appropriate coefficient of pitching moment. During the testing, the shape and position of the wings was changed in order to obtain sufficiently stable model configurations while being manageable. Results were obtained by testing at M=0.35 in the T-35 wind tunnel, at the model rolling angle of ϕ`=0˚, and by CFD simulation at the same conditions. Results are presented by axial force C_A, normal force C_N and pitching moment coefficients C_m. Test results are given for the model aerodynamic center, located at the distance of Xr upstream of the reference plane. The model reference length for the Reynolds number calculation is the diameter of the model.

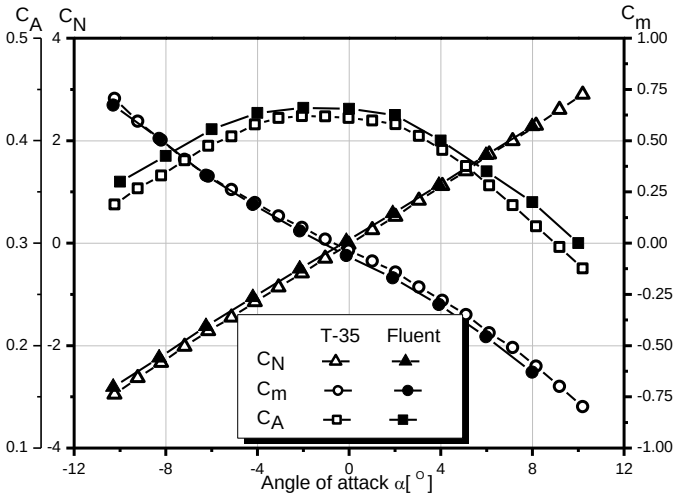

Figure 9. Aerodynamic coefficients of the Original model.

The Original missile model test was used for the aerodynamic coefficient determination, and also for the determination of the aerodynamic characteristics of the common parts for all configurations of the rocket motor section. The relation between the derivatives of the normal force and the pitching moment coefficients was adopted for all new versions of the missile front parts. In the Figure 9 the diagrams of aerodynamic coefficients of the Original model are shown. Having obtained an agreement between the experimental and the numerical results on the Original model configuration, the numerical method was used in the development of the guided missile project with improved front parts.

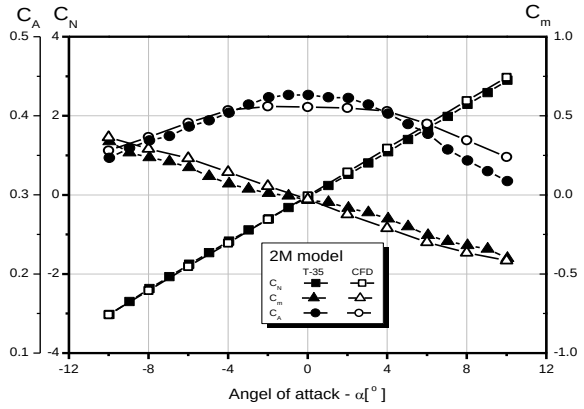

Figure 11. CFD results of the 2M model.

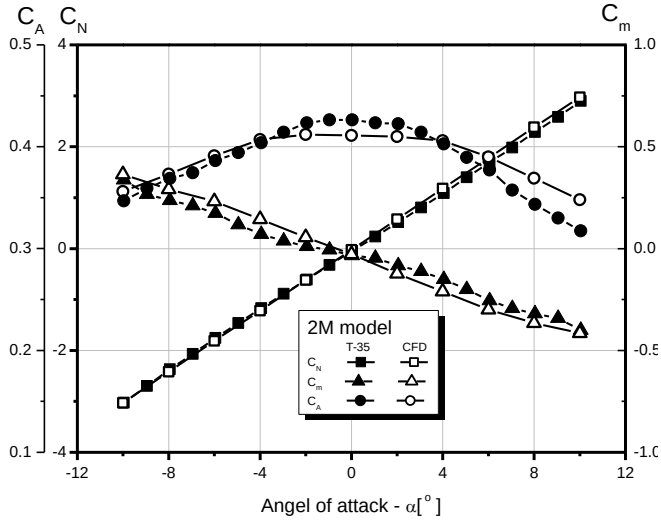

Figure 10. Aerodynamic coeff. of the 2M model.

The results of CFD analysis of the original model was used to adjust the density of the mesh and the layout and setting boundary conditions for models with improved front part. In the Figure 10 the diagrams of aerodynamic coefficients for the 2M model are shown.

During the testing of the 2M model two types of wings were used that were positioned at three locations.

Configuration of the 2M front part with the type B wings at the location C=150mm from the front of the model fulfilled all requirements regarding the relationship between the normal force and the pitching moment coeficient. In the diagrams full symbols mark the final version of the model. The experimentally and numerically obtained results for the 2M model with the type B wings at the location C=150mm were compared, and the comparisons of the coefficients as a function of the model angle of attack are given in graphs in Figure 11. The maximum difference between the calculated and the measured axial force coefficients is about 7.1%.

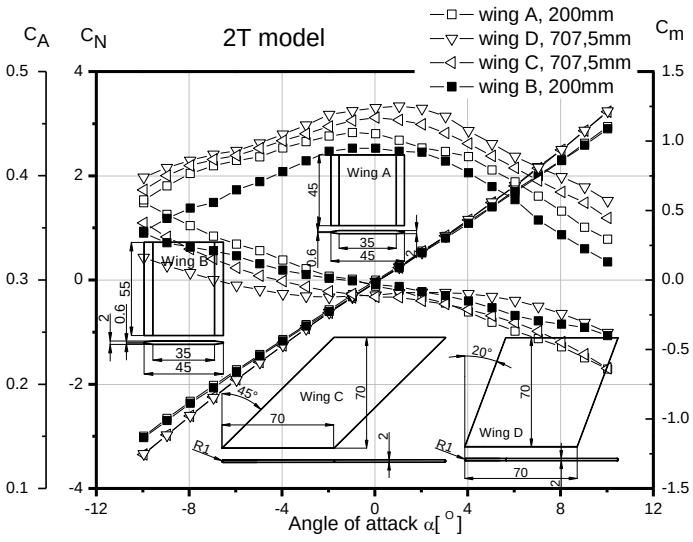

Figure 12. Aerodynamic coeff. of the 2T model.

The maximum difference of the calculated and measured pitching moment coefficients is about 18%. In the Figure 12 the diagrams of aerodynamic coefficients for the 2T model are shown. During the test four types of wings were used that were positioned at two locations. In the Figure 12 the sketch of the four tested wings is also shown. Wings A and B are rectangular 45x45(55) with a diamond cross-sections 2mm thick. Wings C and D are rhombus with sweep angles 45°and 20°, respectively. Cross-section of the wings C and D are rectangular with rounded edges of 0.5mm. Configuration of the 2T front part with the type B wings at the location C=200mm from the front of the model was adopted. The wind tunnel test results and CFD simulation of the 2T model with the type B wings at the location C=200mm were compared in graphs in Figure 13. The maximum difference between the calculated and the measured axial force, normal force and pitching moment coefficients are 10, 2.5 and 4.2%, respectively. In the Figure 14 the diagrams of aerodynamic coefficients for the 2F model are shown. During the test one type of wings was used that was positioned at four locations.

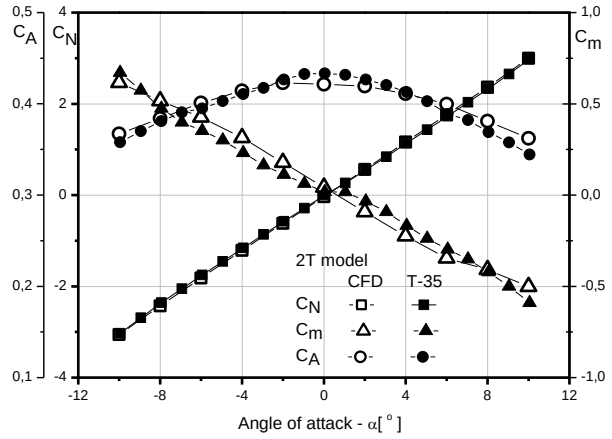

Figure 13. CFD results of the 2T model.

Configuration of the 2F front part with the type A wings at the location C=170mm from the front of the model was adopted. The normal force, pitching moment and axial force coefficients calculated by FLUENT and measured in wind tunnel as a function of the angle of attack for 2F model with the type A wings at the location C=170mm from the front of the model are given in Figure 15.

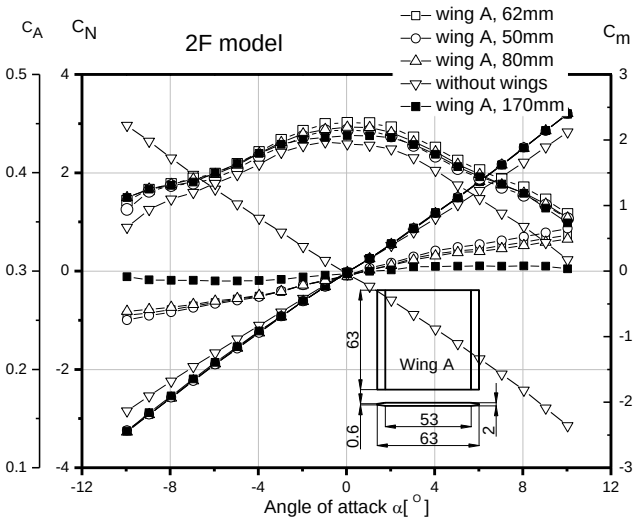

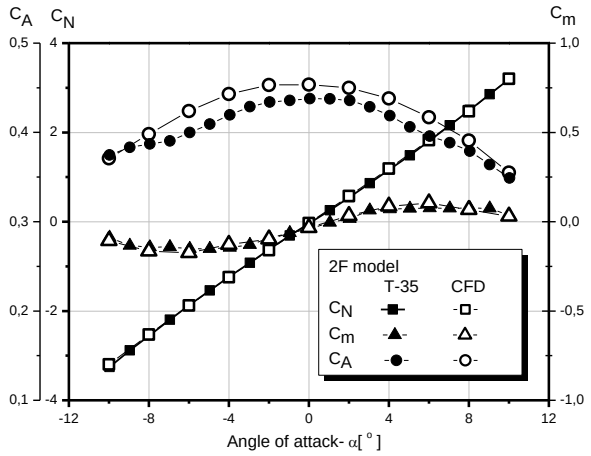

Figure 14. Aerodynamic coeff. of the 2F model.

Figure 15. CFD results of the 2F model.

The maximum difference between the calculated and the measured normal force, pitching moment and axial force, coefficients are 1.8, 12, and 4.8%, respectively. In the Figure 16 and Figure 17 the diagrams of normal force, pitching moment and axial force coefficients for the 2TT and the 2FF model are shown. During the 2TT model test one wing type at one positioned location was used. The number of wings was changed; eight or four wings were used. Configuration of the 2TT front part with

8(eight) wings at the location C=276mm from the front of the model was adopted. During the 2FF model test one wing type positioned at one location C=50mm was used.

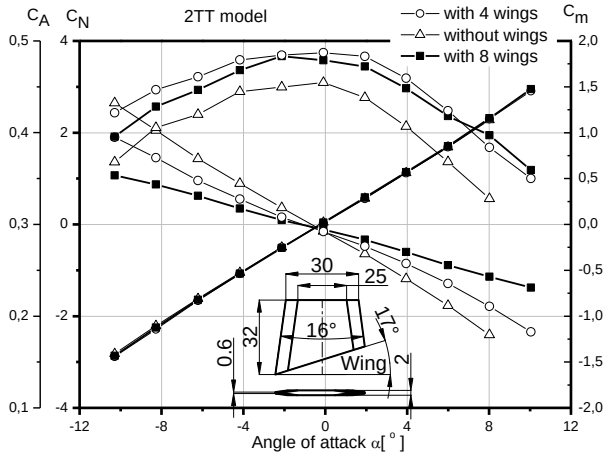

Figure 16. Aerodynamic coeff. of the 2TT model.

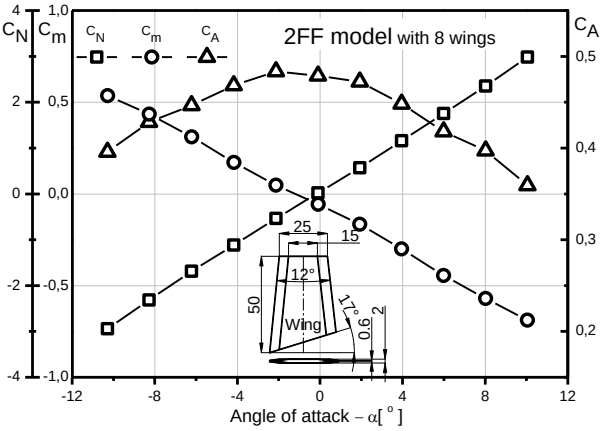

Figure 17. Aerodynamic coeff. of the 2FF model.

Figure 18 shows the dynamic pressure distribution on the GM models body. It can be observed that the dynamic pressure profiles are symmetric in the pitching and yawing plane when AoA=0^{O}.

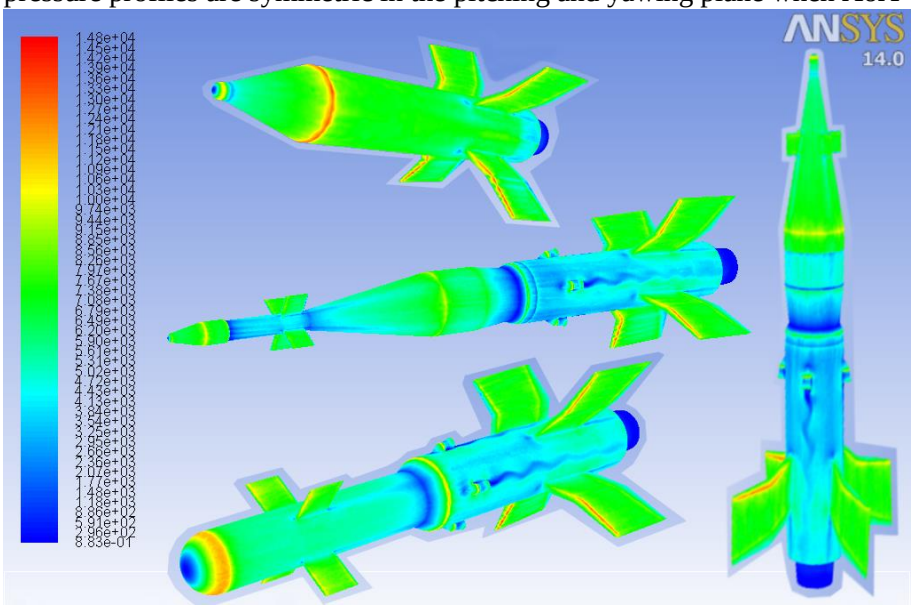

Figure 18. Dynamic pressure distribution on the GM models surface.

In the pressure contour, it can be easily found that there are least dynamic pressure areas at the front of the body, especially in the connecton region of the front part and the rear part of the model and the base of the model. However, the minimum pressure area is also found at the leading edges of the tails. The increase in dynamic pressure can be attributed to the increasing velocity as it moves over the model surface, because the dynamic pressure is a function of the square of velocity. As a result of increase in dynamic pressure, a simultaneous decrease in static pressure results from Bernoulli's theorem or which can also be understood as conservation of the total pressure where, P_0=constant=dynamic+static pressure. The dynamic pressure on the nose is decreasing with increasing angle of attack and the static pressure is increasing with increasing angle of attack. The dynamic pressure on the lower surface is decreasing with increasing angle of attack whereas, the static pressure is increasing on the lower surface. The results of the CFD calculations show good agreement with the results of the wind tunnel experiments for five versions of the GM models and for the original model.

It is also shown that the normal force coefficients of the modified missiles are equal to the normal force coefficients of the original missile. The analysis of the aerodynamic coefficients showed that better agreements between the calculated and the measured aerodynamic coefficients were obtained for the 2T model than for the other models. Practically, there is no difference between the calculated and the measured normal force coefficients for all compared models. The size and shape of the added wings do not influence the normal force coefficients.

5. Discussion

An optimization of the wings' shape and location was performed. The main goal was to maintain the ratio beetwen C_{m_α} and C_{N_α} within the limits ($-0.192 \leq C_{m_\alpha}/C_{N_\alpha} \leq 0.05$), and the second goal to maximize lift to drag ratio C_L/C_D as the original ones. The aerodynamic shape optimization was carried out by varying the shape design variables subject to the slope of the normal force coefficient constraint (C_{N_α}=15.55). The design variables were three external shape variables decisive in shaping the wings i.e. the root chord, tip chord, and span for the all four added wings and also a wing location. The area and sweep-back angle for the wings were determined by a combination of several variables. The design variables in external configuration optimization are defined for wing geometry. These variables are wing leading edge location with respect to the nose tip, semi-span, root chord and the taper ratio of the canard. The upper and lower limits for the variables are defined in a wide range to investigate capabilities of the developed design optimization. Figure 19 represent wing placement area and some possible wing geometries that may be encountered during optimization runs for all five improved front parts.

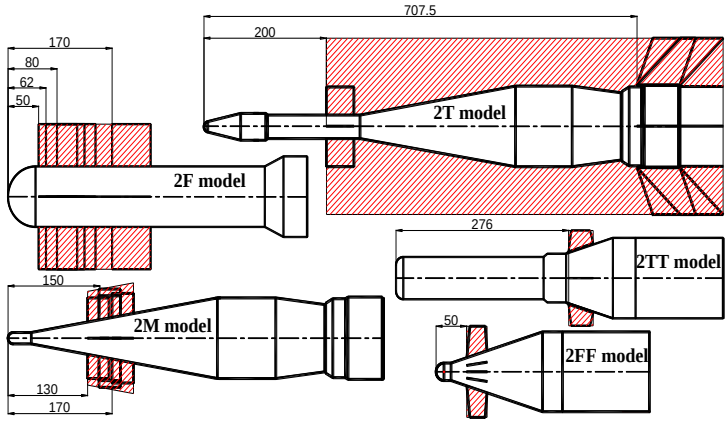

Figure 19. Wing placement area (hatched) and random possible wing geometries

In order to determine the best missile configuration, we created a Pareto front for the optimal results. Therefore, we created 2 graphs in order to better analyze these results. From the Figures 20 and 21 the results for possible combinations of our project target can be seen. For known derivatives of the pitching moment and normal force coefficients ratio of the original missile and assumed required derivatives of the same ratio are determined by changing the wing dimensions and its locations [18-27]. By varying the shape of the missile models, different values of the derivatives of the normal force and pitching moment coefficients are obtained. These analyses revealed a difference between the derivatives for different types of wings. Derivatives of the C_{m_α} and C_{N_α} were obtained from wind tunnel tests, while their required ratio was calculated (Table 2). Optimization was done for about 50 different configurations, but besides the original in the Table 2 only 18 were analyzed and disscussed. The Table 2 shows in bold the chosen shapes for the derivatives ratio optimization derived in this study. The Figure 20 shows the lift to drag ratio versus $C_{m_\alpha}/C_{N_\alpha}$ the ratio for all tested configurations. The hatched area represents the desirable values of the $C_{m_\alpha}/C_{N_\alpha}$ ratio. Five GM models which fulfill the derivatives ratio requirement are marked with full symbols. In was proved by the analysis that there is a small change of the aerodynamic $C_{N\alpha}$ due to the change of the size and the position of the added wings.

Table 2. Estimated aerodynamic characteristics for analyzed model configurations

Mark	Config.	C_{m_α}	C_{N_α}	$C_{m_\alpha}/C_{N_\alpha}$	C_L	C_D	C_L/C_D
O	Original	-2.98	15.55	-0.192	2.82	0.73	3.86
2M	A 150	-4.509	15.88	-0.284	2.78	0.77	3.61
	A 130	-4.592	15.812	-0.290	2.80	0.79	3.54
	A 170	-4.301	16.001	-0.269	2.80	0.78	3.58
	body	-8.797	15.518	-0.567	2.76	0.76	3.60
	B 150	**-1.644**	**17.101**	**-0.096**	**2.80**	**0.81**	**3.47**
2T	A 200	-2.260	15.662	-0.144	2.84	0.84	3.38
	C 707.5	-0.660	16.347	-0.040	3.12	0.90	3.46
	D 707.5	-0.239	17.94	-0.013	3.13	0.92	3.41
	B 200	**-1.165**	**15.931**	**-0.073**	**2.88**	**0.85**	**3.39**
2F	A 62	-4.977	16.392	0.304	3.08	0.88	3.49
	A 50	-5.462	16.428	0.333	3.10	0.88	3.51
	A 80	-4.592	16.221	0.283	3.10	0.88	3.51
	body	-11.29	15.137	-0.746	2.74	0.77	3.54
	A 170	**0.68**	**17.743**	**0.038**	**3.10**	**0.884**	**3.50**
2TT	body	-7.047	14.955	-0.471	2.21	0.63	3.52
	4 wings	-4.474	15.037	-0.298	2.81	0.83	3.38
	8 wings	**-2.998**	**15.501**	**-0.193**	**2.84**	**0.85**	**3.35**
2FF	**8 wings**	**-2.823**	**15.604**	**-0.181**	**2.89**	**0.78**	**3.71**

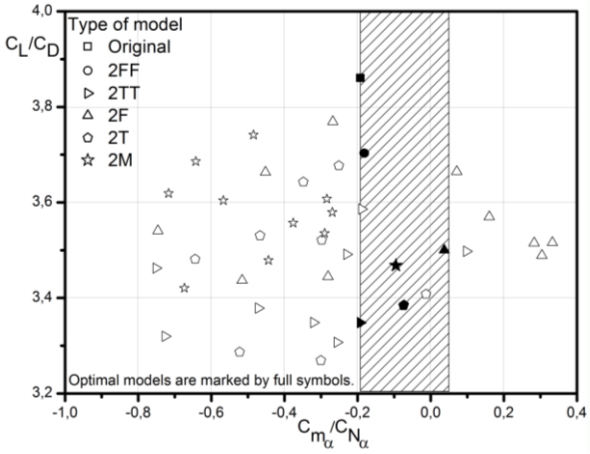

Figure 20. C_L/C_D versus $C_{m_\alpha}/C_{N_\alpha}$ ratio

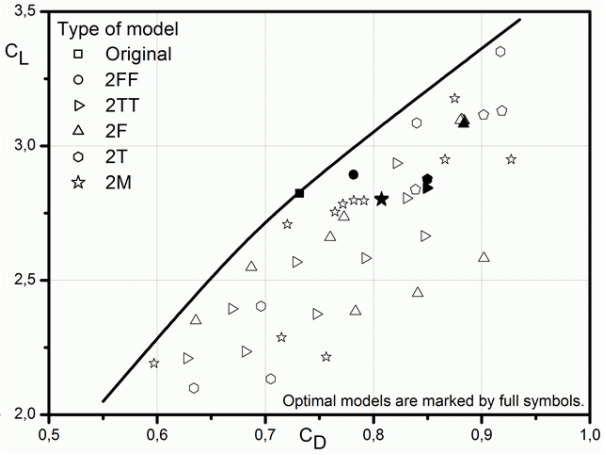

Figure 21. Optimized results for C_L and C_D at fixed α

Figure 21 shows the result of optimization where each point represents a unique shape of the missile. It seems that the pairs of the lift and drag force coefficients were obtained for the same angle of attack for all the configurations considered. The values given for the original (full square) are shown in these graphs to see the relative position between the original and the other configurations. The Figure 21 shows the results for the 2F model as a maximum C_L and C_D configuration, 2M as a minimum C_L and 2FF as a minimum C_D configuration, as well. In terms of the maximum lift to drag ratio the 2FF model is the optimal configuration. In the diagrams full symbols mark the final versions of the model and also the original. Selected configurations have almost the same or slightly better characteristics in terms of maneuverability.

6. Conclusion

The typical conceptual design process for missiles is an iterative process, requiring a number of design iterations to achieve balanced emphasis from the diverse inputs and outputs. Based on requirements, an initial baseline from the existing missiles with a similar mission is established. This baseline is used as a starting point to expedite the missile design convergence. The new conceptual design is evaluated against its flight performance requirements. If the design does not meet the requirements, it is changed and resized for the next iteration and evaluation. If the new missile design

meets the requirements, the design is finalized. Approximately 50 missile shapes were analysed by varying the geometric parameters. Unfortunately, due to wind tunnel testing costs and limited computer resources, we were forced to use only four parameters which describe the wings. These parameters represent the root and tip chord, span and also a wing location.

Results showed that the 2FF configuration is more effective than other configurations. The Pareto optimized configuration was shown to have better aerodynamic features over a range of aerodynamic angles of attack. That is consistently lower drag, while having consistently higher lift and lift-to-drag ratio. The experimentally and numerically obtained results of the aerodynamic coefficients were compared and good agreement was found, so that the designers of the missile projectile had correct guidelines. The existing old generation guided missiles with single shaped-charge warheads have limited applications against modern tanks with reactive armor. In order to overcome this problem, a new range of improved warheads is developed. Partial modernization of the existing GM were done by replacing the existing warheads with new five, more effective, of about 50% greater penetration than the original and slightly greater range. The flight test of the modified versions of the missile proved the validity of the optimization design method given in the paper.

Nomenclature

C_A = axial force coefficient
C_N = normal force coefficient
C_m = pitching moment coefficient
C_L = lift force coefficent
C_D = drag force coefficent
C_L/C_D = lift to drag ratio
C_{m_α} = derivative of pitching moment coeff.
C_{N_α} = derivative of normal force coeff.
L = length of model, m
D = referent length of model, m
S_{ref} = referent area of model, m^2
M = Mach number
p_{st} = static pressure, bar
p_0 = total pressure, bar
q = dynamic pressure, bar
Re = Reynolds number
T_0 = total temperature, K
X_{ref} = distance beetwen point of reduction and virtual center of balance, m
X_r = distance beetwen point of reduction and front of model,m

Greek symbols

α = angle of attack, º
β = sideslip angle, º
ϕ = roll angle, º

Acronyms

F.S. = Transducer full scale
VTI35C = Internal balance ϕ35mm by VTI
VTI = Military Technical Institute
GM = Guided Missile
CFD = Computational Fluid Dynamics

References

[1] Auman, M.L., et al, Aerodynamic characteristics of a guided anti-tank missile utilizing a ram air powered control actuation system, *AIAA*, Reno, USA, 1996.

[2] Anderson, J.,D.,Jr, *Fundamentals of Aerodynamics*, McGraw-Hill, USA, 1991.

[3] Barlow, Jewel, B., et al, *Low Speed Wind Tunnel Testing*, Wiley, New York, 1999.

[4] Katz, J., Plotkin, A., *Low-Speed Aerodynamics*, McGraw-Hill, Singapore, 1991.

[5] Tropea, C., et al, *Springer Handbook of Experimental Fluid Mechanics*, Berlin, 2007.

[6] AIAA Recommended Practice for Wind Tunnel Testing — Part 1, R-092-1-2003e; Part 2, R-092-2-2003e, AIAA Standards, 2003.

[7] AIAA Recommended Practice for Calibration and Use of Internal Strain-Gage Balances with Application to Wind Tunnel Testing, R-091-2003, AIAA Standards, 2003.

[8] Nomenclature and Axis Systems for Aerodynamic Wind Tunnel Testing AIAA G-129-2011, Reston, USA, 2011.

[9] Tuncer, I.,H., et al, Navier–Stokes Analysis of Subsonic Flowfields over a Missile Configuration, *Journal of Spacecraft and Rockets, Vol.35 No.2,* pp 127-131, 1998.

[10] Omar, H. and Abido, M., Multiobjective Evolutionary Algorithm for Designing Fuzzy-Based Missile Guidance Laws." *J. Aerosp. Eng., 24(1),* pp 89–94, 2011.

[11] Blair, A.B.JR, et al, Experimental study of tail-span effects on a canard-controlled missile, *Journal of Spacecraft and Rockets, Vol.30 No.5,* pp 635-640, 1993.

[12] Jong-Eun Kim, *et al*, Development of an efficient aerodynamic shape optimization framework, *Mathematics and Computers in Simulation, Vol.79, No.8,* pp 2373-2384, 2009.

[13] Spirito,J.,D., *et al*,Numerical Investigation of Canard-Controlled Missile with Planar and Grid Fins, *Journal of Spacecraft and Rockets*,Vol.40,No.3,pp363-370, 2003.

[14] Sooy,T.,J., et al, Aerodynamic Predictions, Comparisons, and Validations Using Missile DATCOM(97) and Aeroprediction, *Journal of Space and Rockets,Vol.42,No.2,* pp257-265, 2005.

[15] Doyle,J.,B., Rosema, C.,C., Improved Validation Methodology for Missile Datcom Development, *AIAA*, Orlando, Florida, 2011.

[16] Videnović,N., et al, Validation of the CFD code used for determination of aerodynamic characteristics of non-standard AGARD-B calibration model, *Thermal Science, Vol.18, No.4,* pp 1223-1233, 2014.

[17] Jahangirian, A., Shahrokhi, A., Aerodynamic shape optimization using efficient evolutionary algorithms and unstructured CFD solver, *Computers & Fluids, Vol.46, No.1,* pp 270-276, 2011.

[18] Wei, C., Guo, et al, IFF Optimal Control for Missile Formation Reconfiguration in Cooperative Engagement." *J. Aerosp. Eng., 10.1061/(ASCE)AS.1943-5525.0000359, 04014087,* 2013.

[19] Mao, X. and Yang, S. Optimal Control of Coning Motion of Spinning Missiles, *J. Aerosp. Eng., 28(2), 04014068,* 2015,

[20] B. Rasuo, Scaling between Wind Tunnels-Results Accuracy in Two-Dimensional Testing, *Japan Society of Aeronautical Space Sciences Transactions, 55,* pp 109-115, 2012.

[21] Damljanović, D., et al, T-38 Wind-Tunnel Data Quality Assurance Based on Testing of a Standard Model, *Journal of Aircraft, Vol.50, No.4,* AIAA, pp 1141-1149, 2013.

[22] Ocokoljić, G., Rašuo, B., Testing of the Anti Tank Missile Model with Jets Simulation in the T-35 Subsonic Wind Tunnel, *Scientific Technical Review, Vol.62, No.3-4,* pp 14-20, 2012.

[23] Reuther, J., Jameson, A., Aerodynamic Shape Optimization of Wing and Wing-Body Configurations Using Control Theory, AIAA paper, *33rd Aerospace Sciences Meeting and Exhibit*, Reno, Nevada, January 9-12, 1995.

[24] Baysal, O., Eleshaky, M. E., Aerodynamic design optimization using sensitivity anaysis and computational fluid dynamics, *AIAA Journal,Vol.30,No.3* pp.718-725,doi:10.2514/3.10977, 1992.

[25] Young R. Yang, et al, Aerodynamic Shape Optimization System of a Canard-Controlled Missile Using Trajectory-Dependent Aerodynamic Coefficients, *Journal of Spacecraft and Rockets, Vol. 49, No. 2,* March–April 2012.

[26] Gavrilović, N., et al, Commercial Aircraft Performance Improvement Using Winglets, *FME Transactions, Vol. 43, No1,* pp 1-8, 2015.

[27] Dulikravich, S., G., et al, Automatic Switching Algorithms in Hybrid Single-Objective Optimization, *FME Transactions, Vol. 41, No3,* pp 167-179, 2013.